Long-lived resonances: photonic triangular pyramid

Housni Al-Wahsh, L. Dobrzynski, Abdellatif Akjouj

▶ **To cite this version:**

Housni Al-Wahsh, L. Dobrzynski, Abdellatif Akjouj. Long-lived resonances: photonic triangular pyramid. Photonics and Nanostructures - Fundamentals and Applications, 2022, 50, pp.101022. 10.1016/j.photonics.2022.101022 . hal-03634182

HAL Id: hal-03634182
https://hal.science/hal-03634182v1

Submitted on 22 Jul 2024

HAL is a multi-disciplinary open access archive for the deposit and dissemination of scientific research documents, whether they are published or not. The documents may come from teaching and research institutions in France or abroad, or from public or private research centers.

L'archive ouverte pluridisciplinaire **HAL**, est destinée au dépôt et à la diffusion de documents scientifiques de niveau recherche, publiés ou non, émanant des établissements d'enseignement et de recherche français ou étrangers, des laboratoires publics ou privés.

Distributed under a Creative Commons Attribution - NonCommercial 4.0 International License

Version of Record: https://www.sciencedirect.com/science/article/pii/S1569441022000323
Manuscript_83f7170cf3bfaf2b8bc09d582f529d3d

Long-lived Resonances: Photonic Triangular Pyramid

H. Al-Wahsh
Institut d'Electronique, de Microélectronique et de Nanotechnologie (IEMN),UMR CNRS 8520, Département de Physique, Université de Lille, 59655 Villeneuve d'Ascq Cédex, France and Engineering Mathematics and Physics Department, Faculty of Engineering, Benha University, 11629 Cairo, Egypt

L. Dobrzyński and A. Akjouj
Institut d'Electronique, de Microélectronique et de Nanotechnologie (IEMN),UMR CNRS 8520, Département de Physique, Université de Lille, 59655 Villeneuve d'Ascq Cédex, France

(Dated: 9 March 2022)

New bound in continuum states and long-lived resonances in one photonic triangular pyramid with two semi-infinite leads are reported, together with general theorems giving their existence conditions. The pyramid is composed of connected open loops (of length L). When bound in continuum states exist within state continua, they induce long-lived resonances for specific values of some modified lengths of the 6 open loops constituting the pyramid. This enables to tune these resonances by means of these lengths. The results obtained in this work take due account of the state number conservation between the final system and the reference one constituted by the independent pyramid and semi-infinite leads. The respect of this conservation enables to find all the states of the final system and among them the bound in continuum ones. This is one of the originalities of this work. The other new general results are the different sets of bound in continuum states and long-lived resonances, as well as the theorems giving their existence conditions. These results may have a big impact on general investigations of bound in continuum states, long-lived resonances and communication technology improvements.

Keywords: Photonics, Resonances, Bound in continuum states, Transmission, State Phase

I. INTRODUCTION

Classical and quantum finite systems have discrete states. Without dissipation, the states have an infinite lifetime. A discrete state in interaction with a state continuum induces at least one resonance. It may also remain a discrete bound in continuum (BIC) state[1]. When such a resonance has an infinite decrease at both side of its central wavelength, it is a classical one. When its passing band is confined by one or two zeros, it is a long-lived resonance[2–5].

Recently bound in the continuum states, also known as trapped modes, have brought significant attention due to their important design principle to create systems with long-lived resonances in order to enhance photon-matter interaction[6]. BIC manifests itself as resonances with zero linewidths in lossless systems. They reside within the state continua but remain perfectly confined in some parts of the system (subsystem). BICs was first predicted by Neumann and Wigner in 1929[1]. Since then, BICs were found in various fields of physics such as photonics[7,8], acoustics[9–11], magnonics[12], mesoscopics[13,14] and plasmonics[15–17]. Interest in BICs also results from their potential use in many applications such as lasers[18], filters[19,20] and sensors[21,22]. BICs can be classified into several mechanisms based on their physical origin[6], e.g. symmetry-protected BICs, Fabry-Perot (FP) BICs and Freidrich-Wintgen BICs which have been subsequently investigated theoretically and experimentally in different physical systems[23–26]. BICs modes are not observable from the spectrum due to their irradiative property with vanishing spectral linewidth. However, they can exist only under a specific choice of the material or geometrical parameters of the system. Thus, by slightly detuning the system from the BIC conditions (e.g., changing the geometrical parameters), the latter transforms to a quasi-BIC with a finite width.

The pyramid structure is composed of connected open loops attached to two semi-infinite leads, see Fig.(1). The length of each open loop is L. This system without the leads is shown to have bound in sub-system discrete states. With the leads, some of these states become discrete bound in continuum (BIC) states, or semi-infinite bound in continuum (SIBIC) states. All BIC states may induce, after some symmetry break, long-lived resonances and SIBIC states. These results are obtained with the interface response theory[27] which enables also to deduce the state phase shifts, the variations of the density of states, the transmission, the transmission phase and the transmission phase time. No state can interact with another one through an eigenfunction zero. This fact enables to formulate new SIBIC state and long-lived resonance theorems, in agreement with the BIC[28,29] and activation[28] state ones. These results take due account of the state number conservation between the final sys-

© 2022 published by Elsevier. This manuscript is made available under the CC BY NC user license
https://creativecommons.org/licenses/by-nc/4.0/

tem and the reference one constituted by the independent pyramid and two semi-infinite leads.

This conservation, together with the BIC and SIBIC state theorems, enables to find all the states of the final system and in particular the bound ones. The other new general results are the definition of the SIBIC states and long-lived resonances, together with theorems giving their existence conditions. These general new results are illustrated by original specific ones for the photonic triangular pyramid.

The general starting point is the Maxwell differential propagation equation. So the results of this publication can be transposed to many other physics domains, like phononics, magnonics, electronics, using similar differential equations.

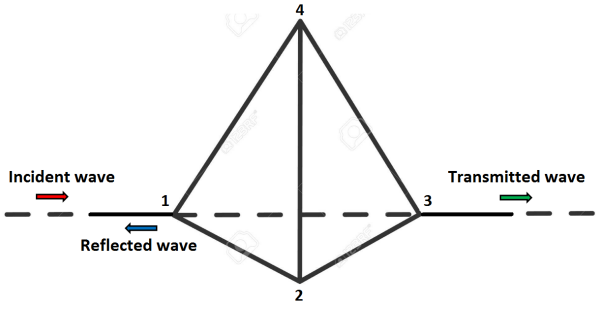

FIG. 1 The pyramid structure studied in this work. The length of each pyramid side is L.

In Sec. II are derived the states of the triangular pyramid (Fig.1) without the leads. Sec. III gives the results obtained for the pyramid with two leads: BIC, SIBIC states and long-lived transmission and reflection resonances. Sec. IV is a summary and a prospective.

II. TRIANGULAR PYRAMID STATES

The simple pyramid structure without the leads described in Fig.(1) is composed of open loops connected together. Use is made of mono-mode guides. The photon wavelengths are large compared to the size of the four pyramid interface sites. Amplification and attenuation can be easily introduced, if needed for comparisons with systems made out of coaxial cables, optical fibers or micro and nano devices.

II.A. Green's function elements

Before giving the states of the triangular pyramid without the leads, we will recall briefly the expression of the Green's function of the different wires (open loops) from which the pyramid structure is composed, namely:

(i) The inverse of the Green's function $[g_L(M_L M_L)]^{-1}$ of a finite segment of length L in the space of its interface $M_L = \{0, L\}$ can be written as a (2×2) matrix[28]

$$[g_L(M_L M_L)]^{-1} = \frac{\alpha}{s}\begin{pmatrix} -c & 1 \\ 1 & -c \end{pmatrix}, \qquad (1)$$

where $c = c(L) = \cos(\alpha L)$, $s = s(L) = \sin(\alpha L)$, $\alpha = 2\pi/\lambda$ and λ is the wavelength.

(ii) The inverse of the Green's (response) function $[g(MM)]^{-1}$ in the space of interface $M = \{1, 2, 3, 4\}$ (Fig.1) of the pyramid structure (without the leads) is given by the linear superposition of the (2×2) matrices given above in Eq.(1) for each of the 6 independent wires (open loops) constituting the pyramid[28]

$$[g(MM)]^{-1} = \frac{\alpha}{s}\begin{pmatrix} -3c & 1 & 1 & 1 \\ 1 & -3c & 1 & 1 \\ 1 & 1 & -3c & 1 \\ 1 & 1 & 1 & -3c \end{pmatrix}. \qquad (2)$$

The boundary conditions are: the continuity of the wave functions and the vanishing at each space point of the sum of the outgoing first derivatives of the field[28]. The eigenfunction derivatives produce source forces. For each eigenstate (resonance), the sum of these forces has to vanish at each space point, concerned by this state[28]. For each state, the sum of all surface forces created by this state, has also to vanish. These conditions are implicitly taken into account in the framework of Interface Response Theory[27].

(iii) The inverse of the Green's function of a semi-infinite wire (lead) is given by[28] $[g_s]^{-1}(M_s M_s) = i\alpha$ where $i = \sqrt{-1}$.

Let us finally mention that the relation of the Green's function elements to the Maxwell differential propagation equation is reported in chapter one of our previous work[28].

II.B. States of the pyramid

The reference system of the pyramid structure is composed here of 6 independent open loops of length L. Therefore the initial states of the system are given by $(\alpha s)^6 = 0$. We have also, for the reference system $[g(MM)]_R^{-1} = (-\alpha^2)^6 = (\alpha^{12})$. The determinant of the matrix given by Eq. (2) is

$$|[g(MM)]^{-1}| = \frac{3\alpha^4(c-1)(3c+1)^3}{s^4}. \qquad (3)$$

So the final states of the system without leads are given by the state number conservation and the state phase shift[28] to be:

$$\alpha^6 s^6 (\frac{3\alpha^4(c-1)(3c+1)^3}{s^4})\alpha^{-12} = 0, \qquad (4)$$

i.e.

$$\alpha^{-2} s^4 (L/2) c^2 (L/2)(3c+1)^3 = 0, \qquad (5)$$

where $c(L/2) = \cos(\alpha L/2)$ and $s(L/2) = \sin(\alpha L/2)$. So the final states of the pyramid are as follows.

For $\alpha = 0$, we have the invariant by translation state $[1, 1, 1, 1]$.

For $s(L/2) = 0$, we have four times degenerate states with $2L/\lambda = 2n, n = 0, 1, 2, 3, ...$. The corresponding eigenvectors are [1,1,1,1], [0,0,0,0], [0,0,0,0], [0,0,0,0]. The

eigenfunction represented by the $[1,1,1,1]$ eigenvector is $\cos(\alpha x)$, where $x=0$ at the first interface point and $\alpha \neq 0$. There are $+\sin(\alpha x)$ or $-\sin(\alpha x)$ between the zeros in the last three eigenvectors, where $x=0$ at the interface points. Each of these three states is confined around one of the four triangles of the pyramid. Each of them is confined in a pyramid subspace and is therefore *a bound in sub-system state*. This sub-system is the triangle in which this state exist. Linear superposition of these three eigenvectors provides a state localized around the fourth triangle.

For $c(L/2)=0$, we have two times degenerate states with eigenvectors [0,0,0,0], [0,0,0,0]. For these two states one has $2L/\lambda = 2n+1, n=0,1,2,\ldots$. Each of the corresponding two eigenvectors is confined around a loop of length $4L$ constituted by two adjacent triangles of the pyramid. Each of them is therefore *a bound in sub-system state*. Here the sub-system is the closed loop 4L.

For $c=-1/3$, we have three times degenerate states, their eigenvectors are $[-1,1,0,0],[-1,0,1,0],[-1,0,0,1]$, or equivalently by linear combination $[-1,1,0,0],[0,-1,1,0],[0,-1,0,1]$. Each of these states is confined within two pyramid triangles.

III. BIC, SIBIC STATES AND TRANSMISSION

III.A. BIC and SIBIC states

According to the above results and to the BIC and SIBIC state theorems given in the Appendix, the structure of Fig. (1) has three BIC states for $s(L/2)=0$ and two BIC states for $c(L/2)=0$. For $c=-1/3$, one has one BIC and two SIBIC states.

The leads attached to sites 1 and 3 transform the pyramid matrix (2) into:

$$[g(MM)]^{-1} = \frac{\alpha}{s}\begin{pmatrix} -3c+is & 1 & 1 & 1 \\ 1 & -3c & 1 & 1 \\ 1 & 1 & -3c+is & 1 \\ 1 & 1 & 1 & -3c \end{pmatrix} \quad (6)$$

Its determinant is:

$$|[g(MM)]^{-1}| = \frac{4\alpha^4}{s^4} s(L/2)[-s(L/2)(1+10c+15c^2) + i(2-3c)(1+3c)c(L/2)]. \quad (7)$$

After due account of the state number conservation and the BIC and SIBIC theorems (see the appendix below), the bound in continuum states of the final system can be confirmed to be given by:

$$s^3(L/2)c^2(L/2)(1+3c)=0. \quad (8)$$

Note that in each of the two reference semi-infinite leads there is only one state for each value of λ[28]. Only a pyramid state with non-zero eigenvector values at the connection points between leads and pyramid interacts with the state continua. The connection of such a pyramid state with the lead states give rise to a resonance peak within the variations of the density of states, and the transmission curves. The incoming and outgoing eigenfunctions in the leads are $\cos(\alpha x)$, where $\alpha = \frac{2\pi}{\lambda}$ and $x=0$ at the interface points between each lead and the pyramid.

III.B. Transmission, transmission phase and state phase shift

Let us consider an incident wave $U(x) = e^{-i\alpha x}$, launched in the left semi-infinite lead (Fig.1). From Eq. (6), one can obtain the transmission function in the right semi-infinite lead, namely, $t_{13} = -2i\alpha g(1,3)$, or equivalently:

$$t_{13} = \frac{-i(1+3c)s}{(c-1)(1+10c+15c^2)+i(2-3c)(1+3c)s} \quad (9)$$

In the same way, the reflection function in the left semi-infinite lead is given by $r_{11} = -1+2i\alpha g(1,1)$. From the expressions of t_{13} (Eq. (9)), one can deduce the transmission coefficient as $T_{13} = |t_{13}|^2$, or equivalently:

$$T_{13} = \frac{2c^2(L/2)(1+3c)^2}{(1+c(3+4c))(-5+c(-20+3c(-5+12c)))}. \quad (10)$$

The transmission coefficient equals zero when $c=-1/3$ and $c(L/2)=0$. The variation of T_{13}, as well as the corresponding reflection coefficient $R_{11} = |r_{11}|^2$ versus $2L/\lambda$ are reported in Fig.(2). The eigen wavelengths of the transmission zeros given by $c=-1/3$ and $c(L/2)=0$ correspond to the eigenmodes of the pyramid without the leads.

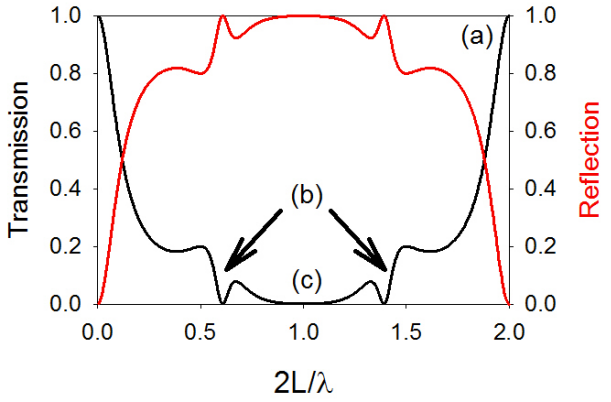

FIG. 2 Transmission (left axis) and Reflection (right axis) vs. $2L/\lambda$ in units without dimension, with: (a) 3 BIC states localized in the pyramid for $s(L/2)=0$. (b) Two SIBIC and one BIC states $c=-1/3$. The corresponding positions of the transmission zeros are: $2L/\lambda = 0.608173, 1.3919, \ldots$. (c) Two BIC states $c(L/2)=0$. The corresponding positions of the transmission zeros are: $2L/\lambda = 1,3,5,\ldots$.

Fig.(2) presents the first period of the transmission (reflection) vs. $2L/\lambda$ in units without dimension. It

repeats periodically to infinity. Note the transmission 1 for $2L/\lambda = 2n, n = 0, 1, 2, ...$ due to the non BIC $s(L/2) = 0$ states. The large highly isolating wavelength band around $2L/\lambda = 1$ is one exceptional result of this triangular pyramid. The two transmission zeros at $2L/\lambda = 0.608173$ and $2L/\lambda = 1.3919$ are obtained from $c = -1/3$, whereas the transmission zero at $2L/\lambda = 1$ is obtained from $c(L/2) = 0$. At the positions indicated on Fig. (2): (a) 3 BIC states localized in the pyramid for $s(L/2) = 0$. (b) Two SIBIC and one BIC state $(1 + 3c) = 0$. (c) Two BIC states $c(L/2) = 0$, the corresponding positions of the transmission zeros are: $2L/\lambda = 1, 3, 5, ...$

The transmission phase is obtained from Eq.(9) to be

$$\phi = tan^{-1}[\frac{-s(L/2)(1 + 10c + 15c^2)}{(2 - 3c)(1 + 3c)c(L/2)}]. \quad (11)$$

Another interesting quantity is the first derivative of ϕ with respect to $2L/\lambda$ which is related to the delay time taken by the photons to traverse the pyramid structure. This quantity, called phase time, is defined by:[30]

$$\tau_\phi = \frac{d\phi}{d(2L/\lambda)} \quad (12)$$

Moreover, another interesting entity that can be extracted from the Green's function is the state phase shift η. The state phase shift between the final system (the pyramid with the leads) and the reference system (the 6 independent open loops and the two semi-infinite leads) is given by[27]:

$$\eta = -arg[det\{g^{-1}(MM)\}] \quad (13)$$

From Eq. (6) one can deduce that:

$$\eta = -tan^{-1}[\frac{(2 - 3c)(1 + 3c)c(L/2)}{-s(L/2)(1 + 10c + 15c^2)}]. \quad (14)$$

In order to provide an analytical comparison of the density of states with the phases involved in the system, we consider the variation of the density of states (VADOS) $\Delta n(2L/\lambda)$ between the final system depicted in Fig. 1 and the reference system composed of the 6 open loops and the two semi-infinite leads. This quantity is given by[27]:

$$\Delta n(2L/\lambda) = -\frac{1}{\pi}\frac{d\eta}{d(2L/\lambda)} \quad (15)$$

Note that the π drops in ϕ and η are due to the zero values of the denominators appearing in their respective analytical expressions. As these denominators are not the same, the η and ϕ, π drop positions are not the same. The positions in η of these π drops are un-shifted for the $s(L/2)$ states and slightly shifted for the others, see Fig. (3).

Fig.(4) presents the variation of the density of states (VADOS) vs. $2L/\lambda$. (a) One negative delta pic due to the loss of the $[1, 1, 1, 1], s(L/2) = 0$ state. (b) The same as (a). (c) Each of the four other negative delta peaks is due to the loss of one bulk state, induced by the SIBIC $[(1 + 3c) = 0]$ states, localized each in one semi-infinite loop and one pyramid closed loop.

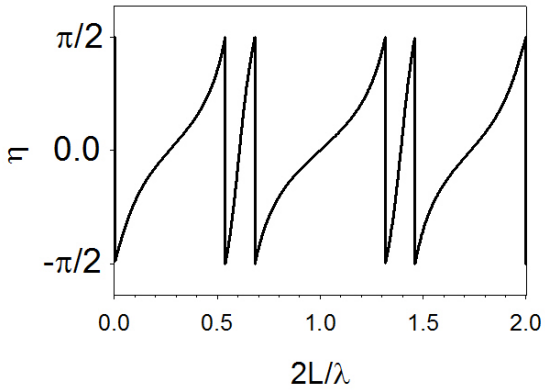

FIG. 3 State phase shift vs. $2L/\lambda$. The two π drops (close to $2L/\lambda = 0.5$) are due to the loss of two bulk states induced by the existence of the two $c = -1/3$ SIBIC states. They produce two resonant peaks. The degeneracy of these peaks is split. Their positions are shifted on each side of the original position. These two peaks superpose exactly and give one single peak in the VADOS. These π drops produce two maxima in the transmission curve (see Fig.(5)).

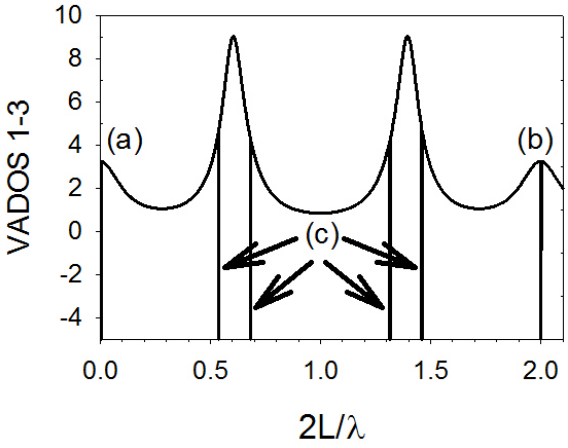

FIG. 4 VADOS vs. $2L/\lambda$. (a) One negative delta pic due to the loss of the $[1, 1, 1, 1], s(L/2) = 0$ state. (b) One negative delta pic due to the loss of the $[1, 1, 1, 1], s(L/2) = 0$ state. (c) Each of the four other negative delta peaks is due to the loss of one bulk state, induced by the SIBIC $[(1 + 3c) = 0]$ states localized each in one semi-infinite loop and one pyramid closed loop.

Fig.(5) presents the VADOS (left axis) and the transmission (right axis) vs. $2L/\lambda$. It stress that all transmission maxima are at the same positions as the π drops, induced by the bulk $[1, 1, 1, 1]$ and the SIBIC states, in the state phase shift. So the existence of the SIBIC states is confirmed by the existence of the corresponding transmission resonances.

Fig.(6) presents the concordance between the VADOS and the state phase shift vs. $2L/\lambda$.

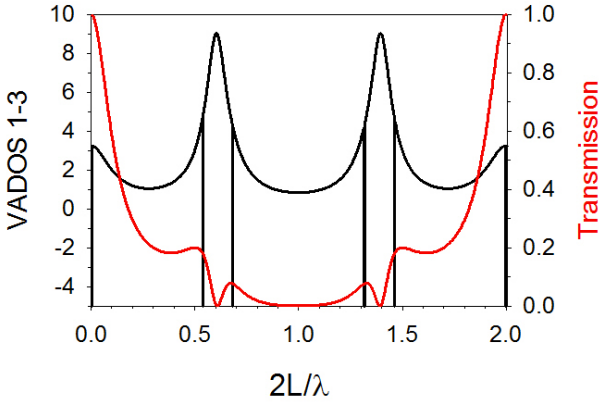

FIG. 5 VADOS (left axis) and Transmission (right axis) vs. $2L/\lambda$. This figure stress that all transmission maxima are at the same positions as the π drops, induced by the bulk $[1,1,1,1]$ and the SIBIC states, in the state phase shift. So the existence of the SIBIC states is confirmed by the existence of the corresponding transmission resonances.

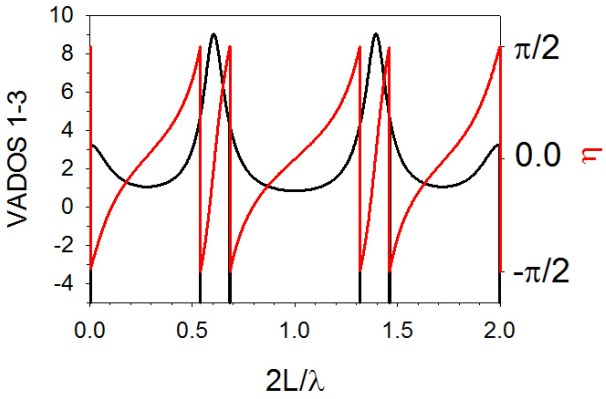

FIG. 6 VADOS (left axis) and state phase shift (right axis) vs. $2L/\lambda$.

Fig.(7) presents the transmission phase (left axis) and transmission (right axis) vs. $2L/\lambda$. The first two π drops from the left are induced by the $c=-1/3$ SIBIC states.

The positions in ϕ of the π drops are much more shifted, see Fig. (7). The most important shift occurs for the reference state $s(L/2)$ with eigenvector $[1,1,1,1]$. The corresponding π drop in ϕ occurs for $c(L/2)=0$. Such shifts happen when one constructs one infinite lead out of two semi-infinite ones[28]. Note also that these π drops, but the $[(2-3c)=0]$ ones, occur for the same wavelengths as the transmission zeros.

Fig.(8) presents the phase time vs. $2L/\lambda$. The phase time and the VADOS are exactly the same, when one neglects the derivatives of the π drops. This happens only when one has two leads. We have also introduced the dissipation in the system by adding a small imaginary part to $2L/\lambda$ i.e., $2L/\lambda$ becomes $2L/\lambda \pm j(0.0001)$. Introducing this imaginary part makes the negative delta peaks show up in the phase time plot.

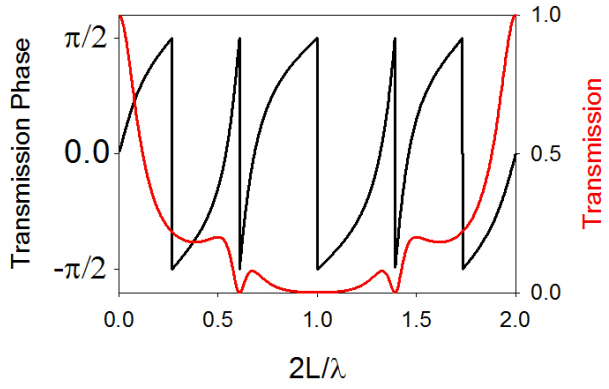

FIG. 7 Transmission phase (left axis) and Transmission (right axis) vs. $2L/\lambda$. The first two pi drops from the left are induced by the $c=-1/3$ SIBIC states. This provides one single peak in the Phase Time, see Fig. (8). The transmission phase exhibits, as predicted, a phase jump at the transmission zeros, and therefore the transmission phase time is different from the density of states.

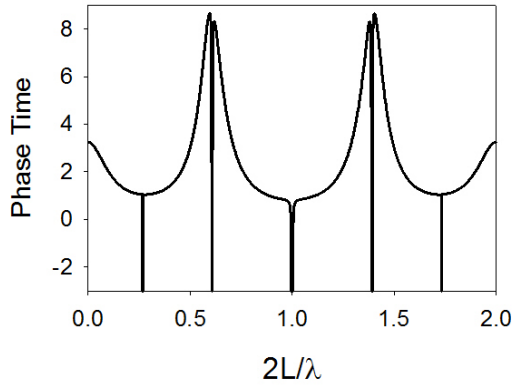

FIG. 8 Phase time vs. $2L/\lambda$. The Phase time and the VADOS are exactly the same, when one neglects the derivatives of the π drops. This happens only when one has two leads. We have also introduced the dissipation in the system by adding a small imaginary part to $2/\lambda$ i.e., $2/\lambda$ becomes $2/\lambda \pm j(0.0001)$. Introducing this imaginary part make the negative delta peaks show up in the phase time plot.

Fig.(9) stress the concordances between the phase time (left axis) and transmission phase (right axis) vs. $2L/\lambda$.

III.C. The long-lived resonances

The above results show the existence of seven BIC states, repeated periodically. Each of them is confined within a different sub-domain closed loop of the triangular pyramid. Four of them induce transmission zeros. The three others coexist at the position of transmission ones.

In what follows are given a few examples of SIBIC states and long-lived resonances induced once some pyra-

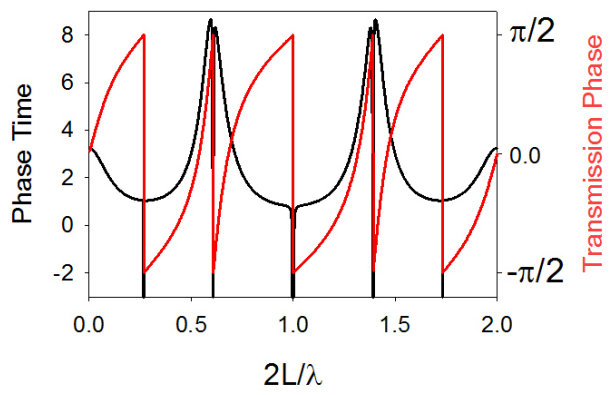

FIG. 9 Phase time (left axis) and Transmission Phase (right axis) vs. $2L/\lambda$.

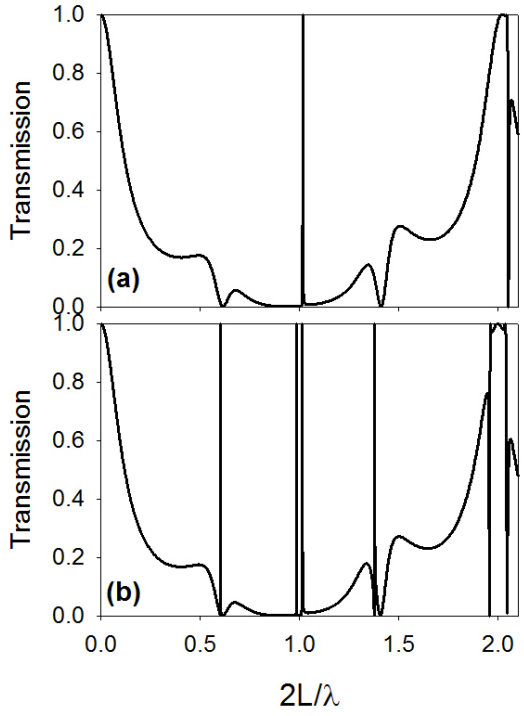

FIG. 10 Transmission (Reflection) vs. $2L/\lambda$. For (a) the parameters are $L_{13} = 0.95, L = 1$. For (b) the parameters are $L_{12} = 1.05, L_{13} = 0.95, L = 1$.

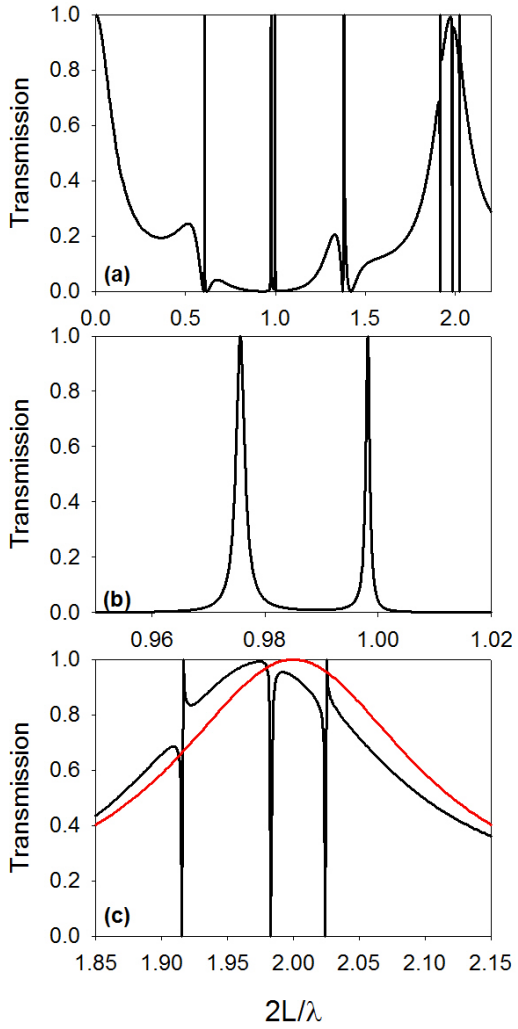

FIG. 11 (a) Transmission vs. $2L/\lambda$ for $L_{12} = 1.05$, $L_{13} = 1.03$, $L_{14} = 1.0$, $L_{23} = 1.05$, $L_{24} = 0.95$, $L_{34} = 1.0$. (b) the same as in (a) but with a zoom enabling to see better the long life resonances near $2L/\lambda = 1$. (c) the same as in (a) but with a zoom enabling to see better the transitions between the three BIC states and the long life resonances near $2L/\lambda = 2$. The resonance existing in the system with all pyramid edge lengths equal to L is in red.

mid symmetries are broken.

a) First consider just a small modification of the distance L_{13} between sites 1 and 3. In the same manner as above, one obtains, after this symmetry break, the states of the pyramid to be given by

$$\alpha^{-2}s^2(L/2)c(L/2)(1+3c)AB = 0, \quad (16)$$

where

$$A = sc(L_{13}/2) + 2cs(L_{13}/2) \quad (17)$$

and

$$B = (3c-1)c(L/2)s(L_{13}/2) + 2s(L/2)c(L_{13}/2)[6c^2(L/2) - 1]. \quad (18)$$

The BIC states of this final system are found to be given by $s(L/2)c(L/2)(1+3c) = 0$. From the numerator of the $g(13)$ element of the response functions of the pyramid, without and with the two leads, one obtains the SIBIC states to be given by $2s(L_{13}) + s(3c-1) = 0$.

Fig. 10 (a) shows an example of the effects observed when the distance L_{13} is slightly modified. Near $2L/\lambda = 1$, one of the two BIC states becomes a sharp long life resonance. Near $2L/\lambda = 2$, one of the two BIC states becomes a sharp anti-resonance.

b) In Fig. (10)(b) L_{12} and L_{13} are both modified. Each

initial $(1 + 3c = 0)$ BIC state induces a sharp long-lived transmission resonance, in between two SIBIC eigenfunction zeros. Note also that the initial transmission zero remains unaffected.

Each initial $(c(L/2) = 0)$ BIC state becomes now a long-lived transmission resonance in between SIBIC eigenfunction zeros.

Near $(2L/\lambda = 2)$, one has now two SIBIC eigenfunction zeros and therefore two long-lived reflection resonances. Long-lived transmission resonances appear also. The left and right ones are induced mostly by a pair of initial BIC and SIBIC states. The central one is induced mostly by the initial bulk and two BIC states.

c) Fig. (11) shows another example for four modified edge lengths.

For the first four from left, long-lived transmission resonances, Fig. 11 (a) and (b) show about the same results as those discussed above on Fig. (10) (b). Let's just stress that the two transmission zeros, for $(1 + 3c = 0)$ remain unaffected by the present stronger symmetry breaks.

The zooms of Fig. 11 (c) enable to see better the transition between the initial three BIC states and the final three reflection and four transmission long-lived resonances, near $2L/\lambda = 2$. These zooms give also in red the resonance existing in the system with all pyramid edge lengths equal to L. Let's stress that the, second from left, transmission long-lived resonance is mostly induced by one initial BIC state (see its first from left peak) and the initial bulk state (see its second peak). It lies between two SIBIC eigenfunction zeros, as does also the, third from left long-lived transmission resonance. The, first and fourth from left, long-lived transmission resonances are respectively on the left and on the right of one SIBIC eigenfunction zero. Note also the existence, in this final perturbed system, of three transmission zeros, near $2L/\lambda = 2$. These transmission zeros are induced by the three SIBIC states. They induce the three reflection long-lived resonances.

All these long-lived resonances agree with the long-lived resonance theorem.

IV. SUMMARY AND PROSPECTIVE

Each BIC state is confined within a finite sub-domain of an infinite system. It induces transmission zeros, but not when another degenerate state with the same wavelength provides a transmission 1.

Each BIC state may be deconfined, by small symmetry breaks, into one long-lived transmission resonance. When this happens, it induces one SIBIC state and one long-lived reflection resonance when it is associated with a degenerate state providing a transmission one. The long-lived reflection resonance appears only when the initial BIC state is degenerate with the same eigenvalue as another bulk state. This bulk state becomes also a long-lived transmission resonance.

A SIBIC state is confined within a semi-infinite subdomain of an infinite system. SIBIC states induce robust transmission zeros, shifted transmission resonances and affect the shape of long-lived resonances close to their robust zeros.

These concepts and the BIC, SIBIC states and long-lived resonance theorems are very general. They may be helpful in wave fundamental and applied investigations, in particular in photonics, phononics, magnonics and electronics. A lot of peculiar BIC, SIBIC states and long-lived resonances remain to be discovered.

ACKNOWLEDGMENTS

The authors thank the referee for his helpful questions. They help to improve this revised manuscript.

H. Al-Wahsh gratefully acknowledge the hospitality of the Institut d'Electronique, de Microélectronique et de Nanotechnologie (IEMN), UMR CNRS 8520 and UFR de Physique, Université de Lille ....

Appendix: GENERAL THEOREMS

No state can interact with another one through an eigenfunction zero. The interaction between two different states implies also the fulfillment of the interface boundary conditions at their connecting interfaces. This enables to obtain the following theorems[28,29], updated here.

1. Bound in continuum(BIC) state

A bound in continuum (BIC) state is a finite subsystem state unconnected with the other bulk states of the final system. Such non connections happen when the connecting space points are eigenfunction nodes and (or) when the eigenfunction general continuity conditions are not fulfilled.

An illustration clarifying the above statement is: if we take into consideration the eigenstate $[-1, 0, 1, 0]$ which belong to the eigenvalue $c = -1/3$ (see section II(B)). This state is one of the degenerate states of the reference finite subsystem (the pyramid with out the leads), see Fig. 12(a). In the final system we attach the two semi-infinite leads at the sites where we have zeros in the eigenvector (namely at the interface sites 2 and 4), see Fig. 12(b). Then this state becomes BIC of the final system (the pyramid with the leads).

2. Semi-infinite BIC (SIBIC) state

A semi infinite bound in continuum (SIBIC) state is a state of a finite subspace connected only with bulk states of a subset of semi-infinite sub-spaces.

The non connections happen when the connecting space points are eigenfunction nodes and (or) when the eigenfunction general continuity conditions are not fulfilled.

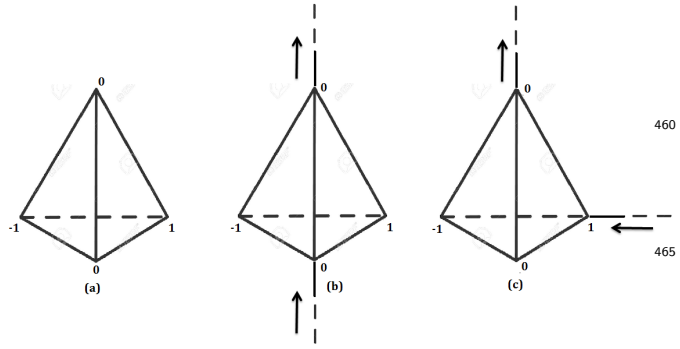

FIG. 12 (a) Reference subsystem with $[-1, 0, 1, 0]$ state. (b) Final system with $[-1, 0, 1, 0]$ as a BIC state. (c) Final system with $[-1, 0, 1, 0]$ as a SIBIC state.

Similar to the illustration given in the above theorem: if in this case we attached one of the leads at a site where we have one and the other lead at a site where we have zero (e.g. at the interface sites 3 and 4) see Fig. 12(c). Then, the state $[-1, 0, 1, 0]$ becomes SIBIC of the final system (the pyramid with the leads).

3. State activation

No state can be activated by actions applied only through its eigenfunction zeros.

4. Long-lived resonance

A small symmetry break of any system may transform a BIC state into a long-lived resonance.

[1] J. von Neuman and E. Wigner, "Uber merkwürdige diskrete Eigenwerte. Uber das Verhalten von Eigenwerten bei adiabatischen Prozessen," Physikalische Zeitschrift **30**, 467–470 (1929).

[2] U. Fano, "Effects of configuration interaction on intensities and phase shifts," Phys. Rev. **124**, 1866–1878 (1961).

[3] M. Fleischhauer, A. Imamoglu, and J. P. Marangos, "Electromagnetically induced transparency: Optics in coherent media," Rev. Mod. Phys. **77**, 633–673 (2005).

[4] J. Jiang, Q. Zhang, Q. Ma, S. Yan, F. Wu, and X. He, "Dynamically tunable electromagnetically induced reflection in terahertz complementary graphene metamaterials," Opt. Mater. Express **5**, 1962–1971 (2015).

[5] Q. Song, L. Ge, J. Wiersig, and H. Cao, "Formation of long-lived resonances in hexagonal cavities by strong coupling of superscar modes," Phys. Rev. A **88**, 023834 (2013).

[6] C. W. Hsu, B. Zhen, A. D. Stone, J. D. Joannopoulos, and M. Soljačić, "Bound states in the continuum," Nature Reviews Materials **1**, 16048 (2016).

[7] A. A. Bogdanov, K. L. Koshelev, P. V. Kapitanova, M. V. Rybin, S. A. Gladyshev, Z. F. Sadrieva, K. B. Samusev, Y. S. Kivshar, and M. F. Limonov, "Bound states in the continuum and Fano resonances in the strong mode coupling regime," Advanced Photonics **1**, 1 (2019).

[8] F. He, J. Liu, G. Pan, F. Shu, X. Jing, and Z. Hong, "Analogue of electromagnetically induced transparency in an all-dielectric double-layer metasurface based on bound states in the continuum," Nanomaterials **11** (2021), 10.3390/nano11092343.

[9] L. Huang, Y. K. Chiang, S. Huang, C. Shen, F. Deng, Y. Cheng, B. Jia, Y. Li, D. A. Powell, and A. E. Miroshnichenko, "Sound trapping in an open resonator," Nature communications **12**, 4819 (2021).

[10] M. Amrani, I. Quotane, C. Ghouila-Houri, E. H. El Boudouti, L. Krutyansky, B. Piwakowski, P. Pernod, A. Talbi, and B. Djafari-Rouhani, "Experimental evidence of the existence of bound states in the continuum and Fano resonances in solid-liquid layered media," Phys. Rev. Applied **15**, 054046 (2021).

[11] I. Quotane, E. H. El Boudouti, and B. Djafari-Rouhani, "Trapped-mode-induced Fano resonance and acoustical transparency in a one-dimensional solid-fluid phononic crystal," Phys. Rev. B **97**, 024304 (2018).

[12] A. Mouadili, E. H. El Boudouti, A. Akjouj, H. Al-Wahsh, B. Djafari-Rouhani, and L. Dobrzynski, "Effect of damping on magnetic induced resonances in cross waveguide structures," Journal of Superconductivity and Novel Magnetism **34**, 597–608 (2021).

[13] T. Mrabti, Z. Labdouti, A. Mouadili, E. El Boudouti, and B. Djafari-Rouhani, "Aharonov-Bohm-effect induced transparency and reflection in mesoscopic rings side coupled to a quantum wire," Physica E: Low-dimensional Systems and Nanostructures **116**, 113770 (2020).

[14] E. N. Bulgakov, K. N. Pichugin, A. F. Sadreev, and I. Rotter, "Bound states in the continuum in open Aharonov-Bohm rings," JETP Lett. **84**, 430 (2006).

[15] S. Sun, Y. Ding, H. Li, P. Hu, C.-W. Cheng, Y. Sang, F. Cao, Y. Hu, A. Alù, D. Liu, Z. Wang, S. Gwo, D. Han, and J. Shi, "Tunable plasmonic bound states in the continuum in the visible range," Phys. Rev. B **103**, 045416 (2021).

[16] Z. Qi, G. Hu, B. Liu, Y. Li, C. Deng, P. Zheng, F. Wang, L. Zhao, and Y. Cui, "Plasmonic nanocavity for obtaining bound state in the continuum in silicon waveguides," Opt. Express **29**, 9312–9323 (2021).

[17] S. Xie, S. Xie, J. Zhan, C. Xie, G. Tian, Z. Li, and Q. Liu, "Bound states in the continuum in a t-shape nanohole array perforated in a photonic crystal slab," Plasmonics **15**, 1261 (2020).

[18] S. T. Ha, Y. H. Fu, N. K. Emani, Z. Pan, R. M. Bakker, R. Paniagua-Domínguez, and A. I. Kuznetsov, "Directional lasing in resonant semiconductor nanoantenna arrays," Nature Nanotechnology **13**, 1042–1047 (2018).

[19] L. L. Doskolovich, E. A. Bezus, and D. A. Bykov, "Integrated flat-top reflection filters operating near bound states in the continuum," Photon. Res. **7**, 1314–1322 (2019).

[20] X. Cui, H. Tian, Y. Du, G. Shi, and Z. Zhou, "Normal incidence filters using symmetry-protected modes in dielectric subwavelength gratings," Scientific Reports **6**, 36066 (2016).

[21] F. Wu, J. Wu, Z. Guo, H. Jiang, Y. Sun, Y. Li, J. Ren, and H. Chen, "Giant enhancement of the goos-hänchen shift assisted by quasibound states in the continuum," Phys. Rev. Applied **12**, 014028 (2019).

[22] D. Conteduca, I. Barth, G. Pitruzzello, C. P. Reardon, E. R. Martins, and T. F. Krauss, "Dielectric nanohole array metasurface for high-resolution near-field sensing and imaging," Nature communications **12**, 3293 (2021).

[23] X. Zhao, C. Chen, K. Kaj, I. Hammock, Y. Huang, R. D. Averitt, and X. Zhang, "Terahertz investigation of bound states in the continuum of metallic metasurfaces," Optica **7**, 1548–1554 (2020).

[24] J. F. Algorri, F. Dell'Olio, P. Roldán-Varona, L. Rodríguez-Cobo, J. M. López-Higuera, J. M. Sánchez-Pena, and D. C. Zografopoulos, "Strongly resonant silicon slot metasurfaces with symmetry-protected bound states in the continuum," Opt. Express **29**, 10374–10385 (2021).

[25] S. I. Azzam, V. M. Shalaev, A. Boltasseva, and A. V. Kildishev, "Formation of bound states in the continuum in hybrid plasmonic-photonic systems," Phys. Rev. Lett. **121**, 253901 (2018).

[26] P. S. Pankin, B. R. Wu, J. H. Yang, K. P. Chen, I. V. Timofeev, and A. F. Sadreev, "One dimensional photonic bound states in the continuum," Communications Physics **3**, 91 (2020).

[27] L. Dobrzynski, A. Akjouj, E. H. El Boudouti, and H. Al-Wahsh et al., "Interface response theory," in *Phononics*, Interface Transmission Tutorial Book Series, edited by L. Dobrzynski (Elsevier, Amsterdam, 2018) pp. 1–18.

[28] L. Dobrzyński, H. Al-Wahsh, A. Akjouj, and E. H. El Boudouti et al., "Photonic paths," in *Photonics*, Interface Transmission

Tutorial Book Series, edited by L. Dobrzyński (Elsevier, 2021) pp. 1–145.

[29] L. Dobrzyński, A. Akjouj, G. Lévêque, E. H. El Boudouti, and H. Al-Wahsh, "Centered system magnons," in *Magnonics*, Interface Transmission Tutorial Book Series, edited by L. Dobrzyński (Elsevier, 2019) pp. 1–51.

[30] M. Büttiker and R. Landauer, "Traversal time for tunneling," Phys. Rev. Lett. **49**, 1739–1742 (1982).